

# Changes of modal properties of simply-supported plane beams due to damages

Zhihai Xiang<sup>†</sup> and Yao Zhang

*Department of Engineering Mechanics, Tsinghua University, Beijing, 100084, P. R. China*

*(Received April 6, 2009, Accepted May 4, 2009)*

**Abstract.** Damage detection methods using structural dynamic responses have received much attention in the past decades. For bridge and offshore structures, these methods are usually based on beam models. To ensure the successful application of these methods, it is necessary to examine the sensitivity of modal properties to structural damages. To this end, an analytic solution is presented of the modal properties of simply-supported Euler-Bernoulli beams that contain a general damage with no additional assumptions. The damage can be a reduction in the bending stiffness or a loss of mass within a beam segment. This solution enables us to thoroughly discuss the sensitivities of different modal properties to various damages. It is observed that the lower natural frequencies and mode shapes do not change so much when a section of the beam is damaged, while the mode of rotation angle and curvature modes show abrupt change near the damaged region. Although similar observations have been reported previously, the analytical solution presented herein for clarifying the mechanism involved is considered a contribution to the literature. It is helpful for developing new damage detection methods for structures of the beam type.

**Keywords:** damage; damage detection; Euler-Bernoulli beam; modal property; sensitivity

---

## 1. Introduction

The aging of important structures, such as bridges, dams and offshore platforms etc., is a hot topic in the civil engineering community and the general public. In order to detect damage occurrences in a timely manner, sensors are often installed in these structures to monitor changes in structural properties. Because structural dynamic properties, such as natural frequencies and mode shapes, can be easily acquired, they are often used as parameters for determining the existence, location and severity of damages (Rizos *et al.* 1990, Salawu 1997, Sinha *et al.* 2002, Owolabi *et al.* 2003, Patil and Maiti 2005). However, some researchers reported that lower natural frequencies and mode shapes are not sensitive to damages (Farrar and Jauregui 1998, Zou *et al.* 2000, Carden and Fanning 2004), due to the fact that the modal data are global properties of a system, while damage is a local phenomenon.

Considering that a better understanding of the relationship between the modal properties and damage is of fundamental importance, some researchers have tried to find the fundamental principles behind. Thomson (1949) presented an analytical solution for slender bars with discontinuities in stiffness. In his model, the slotted bar was replaced by a uniform bar with modified loads at the location of notch.

---

<sup>†</sup> Ph.D., Corresponding Author, Email: [xiangzhihai@tsinghua.edu.cn](mailto:xiangzhihai@tsinghua.edu.cn)

Taking a cracked beam as two beams connected by a rotational spring, Chondros and Dimarogonas (1980) and Rizos *et al.* (1990) presented analytical solutions for the dynamic properties of beams with a transverse surface crack. In their models, the spring constant was obtained from the local flexibility, a function of crack depth (Dimarogonas and Paipetis 1983). Owing to its simplicity, this model is widely accepted by researchers in this field (Dimarogonas 1996, Zheng and Fan 2001, Wang and Qiao 2007). Assuming an exponential stress distribution near the crack, Christides and Barr (1984) studied the dynamic behavior of cracked Euler-Bernoulli beams by the variational principle. This work laid down the foundation of continuous cracked beam theory (Dimarogonas 1996). Various adaptations are developed by the modified energy approach (Sinha *et al.* 2002, Mazanoglu *et al.* 2009). Using the finite element method, Yuen (1985) systematically studied the changes in modal shapes due to the presence of a damage in a cantilever beam. In his model, the damage is introduced by reducing the Young's modulus of some elements. He observed that the rotation of mode shapes or slope of displacement mode shapes are indications for the damage location and severity. Such an observation was also confirmed by Abdo and Hori (2002).

The above researches either using the modified loads to consider a slot in a beam, or the local flexibility to represent cracks existing in a beam, or assuming a stress distribution near the crack, or just using numerical tools such as the finite element method. Although the accuracy of these theories has been proved in part by numerical or experimental means, it is still of some value if a new solution can be developed using the hypotheses of beam theory, but free of any additional assumption. This can be useful to the damage detection of bridge and offshore structures, as they are commonly analyzed by beam models. For this purpose, a new analytical solution will be presented of the modal properties of simply-supported plane Euler-Bernoulli beams with a single general damage in this paper. The damage can be a reduction in bending stiffness or a loss of mass within a beam segment. Based on this solution, a relationship between the modal properties and damage is established for the transverse vibration of the beam. From the examples studied, we observe that: (1) the natural frequencies and mode shapes do not change so much if one section of the beam is damaged; (2) the mode of rotation angle (MRA) shows abrupt change near the damaged location, but relevant indices may incorrectly report damages in the presence of measurement errors; (3) curvature modes are more sensitive to damages than the MRA because they contain more local information. These observations should be useful for developing efficient damage detection method for beam structures.

## 2. Analytical solution of simply-supported plane Euler-Bernoulli beams with a single damage

Fig. 1 shows a simply-supported plane beam of length  $L$  with a single damage in the segment  $l_1 < x \leq l_2$ . The bending stiffnesses of the undamaged and damaged parts are  $(EI)_1$  and  $(EI)_2$ , respectively. The masses per unit length of the undamaged and damaged parts are  $M_1$  and  $M_2$ , respectively. The analytical solution of the natural frequencies and mode shapes of this damaged beam is presented in the following.

### 2.1 Natural frequencies

Using the Euler-Bernoulli beam theory and ignoring the inertial moment caused by angular acceleration, the governing equations for the transverse free vibration of the beam are (Humar 1990):

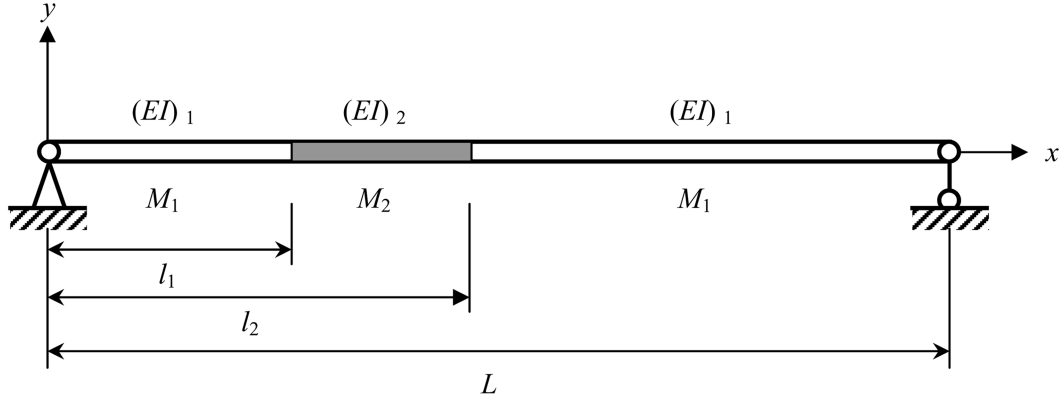


Fig. 1 Simply-supported beam with a single damage

$$M_1 \frac{\partial^2 y}{\partial t^2} + (EI)_1 \frac{\partial^4 y}{\partial x^4} = 0 \quad 0 \leq x \leq l_1, \quad l_2 < x \leq L \quad (1)$$

$$M_2 \frac{\partial^2 y}{\partial t^2} + (EI)_2 \frac{\partial^4 y}{\partial x^4} = 0 \quad l_1 < x \leq l_2 \quad (2)$$

where  $y$  is the transverse displacement and  $t$  denotes time.

Eqs. (1) and (2) can be solved by separation of variables. Assume

$$y(x, t) = Y(x) \sin(\omega t + \varphi) \quad (3)$$

where  $\omega$  is the circular frequency and  $\varphi$  is the initial phase. The mode shape  $Y(x)$  satisfies:

$$\frac{d^4 Y}{dx^4} - K_1^4 Y = 0 \quad 0 \leq x \leq l_1, \quad l_2 < x \leq L \quad (4)$$

$$\frac{d^4 Y}{dx^4} - K_2^4 Y = 0 \quad l_1 < x \leq l_2 \quad (5)$$

where

$$K_1 = \sqrt[4]{\frac{M_1 \omega^2}{(EI)_1}} \quad (6)$$

$$K_2 = \sqrt[4]{\frac{M_2 \omega^2}{(EI)_2}} \quad (7)$$

The general solution of Eqs. (4) and (5) is:

$$Y_1(x) = A_1 \sin K_1 x + B_1 \cos K_1 x + C_1 \sinh K_1 x + D_1 \cosh K_1 x \quad 0 \leq x \leq l_1 \quad (8)$$

$$Y_2(x) = A_2 \sin K_2 x + B_2 \cos K_2 x + C_2 \sinh K_2 x + D_2 \cosh K_2 x \quad l_1 < x \leq l_2 \quad (9)$$

$$Y_3(x) = A_3 \sin K_1 x + B_3 \cos K_1 x + C_3 \sinh K_1 x + D_3 \cosh K_1 x \quad l_2 < x \leq L \quad (10)$$

The constants  $A_i, B_i, C_i, D_i$ , with  $i = 1, 2, 3$ , can be determined from the boundary and continuity conditions as follows:

At  $x = 0$ , the boundary conditions for the simple beam are

$$Y_1(0) = 0 \Rightarrow B_1 + D_1 = 0 \quad (11)$$

$$(EI)_1 Y_1''(0) = 0 \Rightarrow -B_1 + D_1 = 0 \quad (12)$$

From Eqs. (11) and (12), one can get  $B_1 = D_1 = 0$ .

At  $x = L$ , the boundary conditions are

$$Y_3(L) = 0 \Rightarrow A_3 \sin K_1 L + B_3 \cos K_1 L + C_3 \sinh K_1 L + D_3 \cosh K_1 L = 0 \quad (13)$$

$$(EI)_1 Y_3''(L) = 0 \Rightarrow -A_3 \sin K_1 L - B_3 \cos K_1 L + C_3 \sinh K_1 L + D_3 \cosh K_1 L = 0 \quad (14)$$

A superposition of Eq. (13) with Eq. (14) gives

$$C_3 \sinh K_1 L + D_3 \cosh K_1 L = 0 \quad (15)$$

Subtracting Eq. (14) from Eq. (13) gives

$$A_3 \sin K_1 L + B_3 \cos K_1 L = 0 \quad (16)$$

The deflection, rotation angle, bending moment and shear force should be continuous at the position  $x = l_1$ . Because  $B_1 = D_1 = 0$ , the continuity conditions can be written as

$$Y_1(l_1) = Y_2(l_1) \Rightarrow$$

$$A_1 \sin K_1 l_1 + C_1 \sinh K_1 l_1 = A_2 \sin K_2 l_1 + B_2 \cos K_2 l_1 + C_2 \sinh K_2 l_1 + D_2 \cosh K_2 l_1 \quad (17)$$

$$Y_1'(l_1) = Y_2'(l_1) \Rightarrow$$

$$\frac{K_1}{K_2} (A_1 \cos K_1 l_1 + C_1 \cosh K_1 l_1) = A_2 \cos K_2 l_1 - B_2 \sin K_2 l_1 + C_2 \cosh K_2 l_1 + D_2 \sinh K_2 l_1 \quad (18)$$

$$(EI)_1 Y_1''(l_1) = (EI)_2 Y_2''(l_1) \Rightarrow$$

$$\frac{(EI)_1}{(EI)_2} \left( \frac{K_1}{K_2} \right)^2 (-A_1 \sin K_1 l_1 + C_1 \sinh K_1 l_1) = -A_2 \sin K_2 l_1 - B_2 \cos K_2 l_1 + C_2 \sinh K_2 l_1 + D_2 \cosh K_2 l_1 \quad (19)$$

$$(EI)_1 Y_1'''(l_1) = (EI)_2 Y_2'''(l_1) \Rightarrow$$

$$\frac{(EI)_1}{(EI)_2} \left( \frac{K_1}{K_2} \right)^3 (-A_1 \cos K_1 l_1 + C_1 \cosh K_1 l_1) = -A_2 \cos K_2 l_1 - B_2 \sin K_2 l_1 + C_2 \cosh K_2 l_1 + D_2 \sinh K_2 l_1 \quad (20)$$

Similarly, at  $x = l_2$ , the continuity conditions are

$$\begin{aligned} Y_2(l_2) = Y_3(l_2) &\Rightarrow A_2 \sin K_2 l_2 + B_2 \cos K_2 l_2 + C_2 \sinh K_2 l_2 + D_2 \cosh K_2 l_2 \\ &= A_3 \sin K_1 l_2 + B_3 \cos K_1 l_2 + C_3 \sinh K_1 l_2 + D_3 \cosh K_1 l_2 \end{aligned} \quad (21)$$

$$A_2 \cos K_2 l_2 - B_2 \sin K_2 l_2 + C_2 \cosh K_2 l_2 + D_2 \sinh K_2 l_2$$

$$Y_2'(l_2) = Y_3'(l_2) \Rightarrow = \frac{K_1}{K_2} (A_3 \cos K_1 l_2 - B_3 \sin K_1 l_2 + C_3 \cosh K_1 l_2 + D_3 \sinh K_1 l_2) \quad (22)$$

$$(EI)_2 Y_2''(l_2) = (EI)_1 Y_3''(l_2) \Rightarrow -A_2 \sin K_2 l_2 - B_2 \cos K_2 l_2 + C_2 \sinh K_2 l_2 + D_2 \cosh K_2 l_2$$

$$= \frac{(EI)_1}{(EI)_2} \left( \frac{K_1}{K_2} \right)^2 (-A_3 \sin K_1 l_2 - B_3 \cos K_1 l_2 + C_3 \sinh K_1 l_2 + D_3 \cosh K_1 l_2) \quad (23)$$

$$(EI)_2 Y_2'''(l_2) = (EI)_1 Y_3'''(l_2) \Rightarrow -A_2 \cos K_2 l_2 + B_2 \sin K_2 l_2 + C_2 \cosh K_2 l_2 + D_2 \sinh K_2 l_2$$

$$= \frac{(EI)_1}{(EI)_2} \left( \frac{K_1}{K_2} \right)^3 (-A_3 \cos K_1 l_2 + B_3 \sin K_1 l_2 + C_3 \cosh K_1 l_2 + D_3 \sinh K_1 l_2) \quad (24)$$

Eq. (15) through Eq. (24) can be rewritten in matrix form as

$$\begin{bmatrix} \mathbf{a}_{11} & \mathbf{a}_{12} & \mathbf{a}_{13} \\ \mathbf{a}_{21} & \mathbf{a}_{22} & \mathbf{a}_{23} \\ \mathbf{a}_{31} & \mathbf{a}_{32} & \mathbf{a}_{33} \end{bmatrix} \begin{Bmatrix} \mathbf{b}_1 \\ \mathbf{b}_2 \\ \mathbf{b}_3 \end{Bmatrix} = \mathbf{0} \quad (25a)$$

where  $\mathbf{b}_1 = (A_1 \ C_1)^T$ ,  $\mathbf{b}_2 = (A_2 \ B_2 \ C_2 \ D_2)^T$ ,  $\mathbf{b}_3 = (A_3 \ B_3 \ C_3 \ D_3)^T$  and sub-matrices  $\mathbf{a}_{ij}$  ( $i, j = 1, 2, 3$ ) are

$$\mathbf{a}_{11} = \begin{bmatrix} \sin K_1 l_1 & \sinh K_1 l_1 \\ r \cos K_1 l_1 & r \cosh K_1 l_1 \end{bmatrix} \quad (25b)$$

$$\mathbf{a}_{12} = \begin{bmatrix} -\sin K_2 l_1 & -\cos K_2 l_1 & -\sinh K_2 l_1 & -\cosh K_2 l_1 \\ -\cos K_2 l_1 & \sin K_2 l_1 & -\cosh K_2 l_1 & -\sinh K_2 l_1 \end{bmatrix} \quad (25c)$$

$$\mathbf{a}_{13} = \begin{bmatrix} 0 & 0 & 0 & 0 \\ 0 & 0 & 0 & 0 \end{bmatrix} \quad (25d)$$

$$\mathbf{a}_{21} = \begin{bmatrix} -sr^2 \sin K_1 l_1 & sr^2 \sinh K_1 l_1 \\ -sr^3 \cos K_1 l_1 & sr^3 \cosh K_1 l_1 \\ 0 & 0 \\ 0 & 0 \end{bmatrix} \quad (25e)$$

$$\mathbf{a}_{22} = \begin{bmatrix} \sin K_2 l_1 & \cos K_2 l_1 & -\sinh K_2 l_1 & -\cosh K_2 l_1 \\ \cos K_2 l_1 & -\sin K_2 l_1 & -\cosh K_2 l_1 & -\sinh K_2 l_1 \\ \sin K_2 l_2 & \cos K_2 l_2 & \sinh K_2 l_2 & \cosh K_2 l_2 \\ \cos K_2 l_2 & -\sin K_2 l_2 & \cosh K_2 l_2 & \sinh K_2 l_2 \end{bmatrix} \quad (25f)$$

$$\mathbf{a}_{23} = \begin{bmatrix} 0 & 0 & 0 & 0 \\ 0 & 0 & 0 & 0 \\ -\sin K_1 l_2 & -\cos K_1 l_2 & -\sinh K_1 l_2 & -\cosh K_1 l_2 \\ -r \cos K_1 l_2 & r \sin K_1 l_2 & -r \cosh K_1 l_2 & -r \sinh K_1 l_2 \end{bmatrix} \quad (25g)$$

$$\mathbf{a}_{31} = \begin{bmatrix} 0 & 0 \\ 0 & 0 \\ 0 & 0 \\ 0 & 0 \end{bmatrix} \quad (25h)$$

$$\mathbf{a}_{32} = \begin{bmatrix} -\sin K_2 l_2 & -\cos K_2 l_2 & \sinh K_2 l_2 & \cosh K_2 l_2 \\ -\cos K_2 l_2 & \sin K_2 l_2 & \cosh K_2 l_2 & \sinh K_2 l_2 \\ 0 & 0 & 0 & 0 \\ 0 & 0 & 0 & 0 \end{bmatrix} \quad (25i)$$

$$\mathbf{a}_{33} = \begin{bmatrix} sr^2 \sin K_1 l_2 & sr^2 \cos K_1 l_2 & -sr^2 \sinh K_1 l_2 & -sr^2 \cosh K_1 l_2 \\ sr^3 \cos K_1 l_2 & -sr^3 \sin K_1 l_2 & -sr^3 \cosh K_1 l_2 & -sr^3 \sinh K_1 l_2 \\ \sin K_1 L & \cos K_1 L & 0 & 0 \\ 0 & 0 & \sinh K_1 L & \cosh K_1 L \end{bmatrix} \quad (25j)$$

In Eq. (25b) through Eq. (25j)

$$s = \frac{(EI)_1}{(EI)_2} \quad (25k)$$

$$r = \frac{K_1}{K_2} = \sqrt[4]{\frac{(EI)_2 M_1}{(EI)_1 M_2}} \quad (25l)$$

For Eq. (25) to have nontrivial solutions, the determinant of its coefficient matrix should equal zero. Denote

$$R_l = \frac{l_1}{L} \quad (26)$$

$$R_d = \frac{l_2 - l_1}{L} \quad (27)$$

and define

$$a = K_2 l_1 - K_1 L + K_1 l_2 + K_1 l_1 - K_2 l_2 = K_1 L \left[ 2R_l - 1 + \left(1 - \frac{1}{r}\right) R_d \right] \quad (28)$$

$$b = K_2 l_1 + K_1 L - K_1 l_2 + K_1 l_1 - K_2 l_2 = K_1 L \left[ 1 - \left(1 + \frac{1}{r}\right) R_d \right] \quad (29)$$

$$c = -K_2l_1 + K_1L - K_1l_2 + K_1l_1 + K_2l_2 = K_1L \left[ 1 - \left( 1 - \frac{1}{r} \right) R_d \right] \quad (30)$$

$$d = -K_2l_1 - K_1L + K_1l_2 + K_1l_1 + K_2l_2 = K_1L \left[ 2R_l - 1 + \left( 1 + \frac{1}{r} \right) R_d \right] \quad (31)$$

$$e = -K_1l_2 + K_1l_1 + K_1L = K_1L(1 - R_d) \quad (32)$$

$$f = K_1l_2 + K_1l_1 - K_1L = K_1L(2R_l - 1 + R_d) \quad (33)$$

The determinant of the coefficient matrix of Eq. (25) can be obtained as

$$\begin{aligned} & [(1 + r^2s)^4 - 4r^2s^2(1 + r^2)^2](\sin a \sinh a + \sin d \sinh d) - [(1 + r^2s)^2 - 2rs(1 + r^2)]^2 \sin b \sinh b \\ & - [(1 + r^2s)^2 + 2rs(1 + r^2)]^2 \sin c \sinh c + 4(r^4s^2 - 1)^2(\sin e \sin e - \sin f \sinh f + \cos e \cosh f - \cos f \cosh e) \\ & + 2rs(r^2 - 1) \{ [(1 + r^2s)^2 - 2rs(1 + r^2)] [\sin a \sinh b + \sin b(\sinh a - \sinh d) - \sin d \sinh b] + \\ & \quad [(1 + r^2s)^2 + 2rs(1 + r^2)] [\sin a \sinh c + \sin c(\sinh a - \sinh d) - \sin d \sinh c] \} \\ & + [(r^4s^2 - 1)^2 + 4r^2s(1 - r^4s)(s - 1)](\sin a \sinh d + \sin d \sinh a) - [(r^2s - 1)^4 - 4r^2s^2(1 - r^2)^2] \\ & \quad (\sin b \sinh c + \sin c \sinh b) \\ & + (r^2s - 1)^2 \{ [(1 + r^2s)^2 - 2rs(1 + r^2)] [\cos a \cosh b - \cos b(\cosh a + \cosh d) + \cos d \cosh b] + \\ & \quad [(1 + r^2s)^2 + 2rs(1 + r^2)] [\cos a \cosh c - \cos c(\cosh a + \cosh d) + \cos d \cosh c] \} \\ & + 4rs(r^2 - 1)(r^2s - 1)^2(\cos b \cosh c - \cos c \cosh b) = 0 \end{aligned} \quad (34)$$

For a given damage, i.e., fixed values of  $R_l$ ,  $R_d$ ,  $s$  and  $r$ , Eq. (34) is a transcendental equation with only one unknown  $K_1L$ . This equation can be easily solved by numerical methods. After obtaining a solution of  $K_1L$ , the  $n$ th natural frequency can be calculated according to Eqs. (6) and (7)

$$f_d = \frac{(K_1L)_n^2}{2\pi L^2} \sqrt{\frac{(EI)_1}{M_1}}, \quad n = 1, 2, 3, \dots \quad (35)$$

For the case where there is no damage, the above equations degenerate to the well-known solution of free vibration for simply-supported beams (see Appendix for details).

## 2.2 Mode shapes

When Eq. (34) is satisfied, an infinite number of solutions can be obtained from Eq. (25). To obtain the  $n$ th mode shape, we can use  $A_3$  to represent all nonzero constants as follows:

$$A_1 = A_3 \frac{(sr^2 + 1)^2 \Delta_1 + (sr^2 - 1)^2 \Delta_5 + (s^2 r^4 - 1)(\Delta_2 + \Delta_6) \Theta}{4sr^2 \sin K_1 l_1} \quad (36)$$

$$C_1 = A_3 \frac{(s^2 r^4 - 1)(\Delta_1 + \Delta_5) + [(sr^2 - 1)^2 \Delta_2 + (sr^2 + 1)^2 \Delta_6] \Theta}{4sr^2 \sinh K_1 l_1} \quad (37)$$

$$A_2 = \frac{A_3}{2} [(sr^2 + 1)(\Phi_1 \sin K_2 l_2 + r\Phi_3 \cos K_2 l_2) - (sr^2 - 1)(\Phi_2 \sin K_2 l_2 + r\Phi_4 \cos K_2 l_2) \Theta] \quad (38)$$

$$B_2 = \frac{A_3}{2} [(sr^2 + 1)(\Phi_1 \cos K_2 l_2 - r\Phi_3 \sin K_2 l_2) - (sr^2 - 1)(\Phi_2 \cos K_2 l_2 - r\Phi_4 \sin K_2 l_2) \Theta] \quad (39)$$

$$C_2 = \frac{A_3}{2} [(sr^2 - 1)(\Phi_1 \sinh K_2 l_2 - r\Phi_3 \cosh K_2 l_2) - (sr^2 + 1)(\Phi_2 \sinh K_2 l_2 - r\Phi_4 \cosh K_2 l_2) \Theta] \quad (40)$$

$$D_2 = \frac{A_3}{2} [-(sr^2 - 1)(\Phi_1 \cosh K_2 l_2 - r\Phi_3 \sinh K_2 l_2) + (sr^2 + 1)(\Phi_2 \cosh K_2 l_2 - r\Phi_4 \sinh K_2 l_2) \Theta] \quad (41)$$

$$B_3 = -A_3 \operatorname{tg} K_1 L \quad (42)$$

$$C_3 = A_3 \Theta \quad (43)$$

$$D_3 = -A_3 \Theta \tanh K_1 L \quad (44)$$

where

$$\Phi_1 = \sin K_1 l_2 - \operatorname{tg} K_1 L \cos K_1 l_2 \quad (45)$$

$$\Phi_2 = \sinh K_1 l_2 - \tanh K_1 L \cosh K_1 l_2 \quad (46)$$

$$\Phi_3 = \cos K_1 l_2 + \operatorname{tg} K_1 L \sin K_1 l_2 \quad (47)$$

$$\Phi_4 = \cosh K_1 l_2 - \tanh K_1 L \sinh K_1 l_2 \quad (48)$$

$$\Delta_1 = (\Phi_1 \sin K_2 l_2 + r\Phi_3 \cos K_2 l_2) \sin K_2 l_1 + (\Phi_1 \cos K_2 l_2 - r\Phi_3 \sin K_2 l_2) \cos K_2 l_1 \quad (49)$$

$$\Delta_2 = -(\Phi_2 \sin K_2 l_2 + r\Phi_4 \cos K_2 l_2) \sin K_2 l_1 - (\Phi_2 \cos K_2 l_2 - r\Phi_4 \sin K_2 l_2) \cos K_2 l_1 \quad (50)$$

$$\Delta_3 = (\Phi_1 \sin K_2 l_2 + r\Phi_3 \cos K_2 l_2) \cos K_2 l_1 - (\Phi_1 \cos K_2 l_2 - r\Phi_3 \sin K_2 l_2) \sin K_2 l_1 \quad (51)$$

$$\Delta_4 = -(\Phi_2 \sin K_2 l_2 + r\Phi_4 \cos K_2 l_2) \cos K_2 l_1 + (\Phi_2 \cos K_2 l_2 - r\Phi_4 \sin K_2 l_2) \sin K_2 l_1 \quad (52)$$

$$\Delta_5 = (\Phi_1 \sinh K_2 l_2 - r\Phi_3 \cosh K_2 l_2) \sinh K_2 l_1 - (\Phi_1 \cosh K_2 l_2 - r\Phi_3 \sinh K_2 l_2) \cosh K_2 l_1 \quad (53)$$

$$\Delta_6 = -(\Phi_2 \sinh K_2 l_2 - r\Phi_4 \cosh K_2 l_2) \sinh K_2 l_1 + (\Phi_2 \cosh K_2 l_2 - r\Phi_4 \sinh K_2 l_2) \cosh K_2 l_1 \quad (54)$$

$$\Delta_7 = (\Phi_1 \sinh K_2 l_2 - r\Phi_3 \cosh K_2 l_2) \cosh K_2 l_1 - (\Phi_1 \cosh K_2 l_2 - r\Phi_3 \sinh K_2 l_2) \sinh K_2 l_1 \quad (55)$$

$$\Delta_8 = -(\Phi_2 \sinh K_2 l_2 - r\Phi_4 \cosh K_2 l_2) \cosh K_2 l_1 + (\Phi_2 \cosh K_2 l_2 - r\Phi_4 \sinh K_2 l_2) \sinh K_2 l_1 \quad (56)$$

$$\Theta = \frac{(s^2 r^4 - 1) \left[ (\Delta_1 + \Delta_5) - (\Delta_3 + \Delta_7) \frac{\tanh K_1 l_1}{r} \right]}{(sr^2 - 1)^2 \left( \Delta_4 \frac{\tanh K_1 l_1}{r} - \Delta_2 \right) + (sr^2 + 1)^2 \left( \Delta_8 \frac{\tanh K_1 l_1}{r} - \Delta_6 \right)} \quad (57)$$

### 3. Influence of damage on modal properties

In this section, we shall check the validity of the above analytical solution for the natural frequencies and mode shapes by comparing it with the finite element results. The influence of damages on the two modal properties will be evaluated simultaneously. Then, based on the analytical solution, some examples will be adopted to study the sensitivity of the MRA and curvature modes to damage, and the influence of measurement errors.

#### 3.1 Influence on natural frequencies

For the purpose of validating the analytical solution, we adopt a simply-supported beam with a square cross-section. Suppose the beam length is  $L = 100$  m, the dimension of the beam cross-section is  $1 \times 1$  m, Young's modulus  $E = 2.1 \times 10^{11}$  Pa and the beam density is  $\rho = 7000$  kg/m<sup>3</sup>. The damage is defined as a transverse double-sided slot of width  $l_2 - l_1$  and height  $1 - h$ , located a distance  $l_1$  from the left support (see Fig. 2).

For this damaged beam,  $s = \frac{(EI)_1}{(EI)_2} = \frac{1}{h^3}$ ,  $r = \sqrt[4]{\frac{(EI)_2 M_1}{(EI)_1 M_2}} = \sqrt{h}$ . Thus, Eq. (34) becomes

$$\begin{aligned}
& \left[ \left(1 + \frac{1}{h^2}\right)^4 - \frac{4}{h^5}(1+h)^2 \right] (\sin a \sinh a + \sin d \sinh d) - \left[ \left(1 + \frac{1}{h^2}\right)^2 - 2\frac{\sqrt{h}}{h^3}(1+h) \right]^2 \sin b \sinh b \\
& - \left[ \left(1 + \frac{1}{h^2}\right)^2 + 2\frac{\sqrt{h}}{h^3}(1+h) \right]^2 \sin c \sinh c + 4\left(\frac{1}{h^4} - 1\right)^2 [(\sin e \sinh e - \sin f \sinh f + \cos e \cosh e - \cos f \cosh f)] + \\
& + 2\frac{\sqrt{h}}{h^3}(h-1) \left\{ \left[ \left(1 + \frac{1}{h^2}\right)^2 - 2\frac{\sqrt{h}}{h^3}(1+h) \right] [\sin a \sinh b + \sin b(\sinh a - \sinh d) - \sin d \sinh b] + \right. \\
& \quad \left. \left[ \left(1 + \frac{1}{h^2}\right)^2 + 2\frac{\sqrt{h}}{h^3}(1+h) \right] [\sin a \sinh c + \sin c(\sinh a - \sinh d) - \sin d \sinh c] \right\} \\
& + \left[ \left(\frac{1}{h^4} - 1\right)^2 + \frac{4}{h^2} \left(1 - \frac{1}{h}\right) \left(\frac{1}{h^3} - 1\right) \right] (\sin a \sinh d + \sin d \sinh a) - \left[ \left(\frac{1}{h^2} - 1\right)^4 - \frac{4}{h^5}(1-h)^2 \right] \\
& \quad (\sin b \sinh c + \sin c \sinh b) \\
& + \left(\frac{1}{h^2} - 1\right)^2 \left\{ \left[ \left(1 + \frac{1}{h^2}\right)^2 - 2\frac{\sqrt{h}}{h^3}(1+h) \right] [\cos a \cosh b - \cos b(\cosh a + \cosh d) + \cos d \cosh b] + \right. \\
& \quad \left. \left[ \left(1 + \frac{1}{h^2}\right)^2 + 2\frac{\sqrt{h}}{h^3}(1+h) \right] [\cos a \cosh c - \cos c(\cosh a + \cosh d) + \cos d \cosh c] \right\} \\
& + 4\frac{\sqrt{h}}{h^3}(h-1) \left(\frac{1}{h^2} - 1\right)^2 (\cos b \cosh c - \cos c \cosh b) = 0 \tag{58}
\end{aligned}$$

According to Eq. (28) through Eq. (33), the variables in the above equation can be written as:

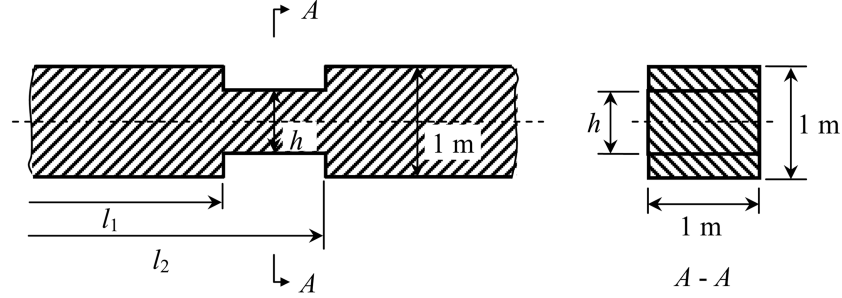


Fig. 2 Damaged segment with transverse double-sided slot in width

$$a = K_1 L \left[ 2R_l - 1 + \left( 1 - \frac{1}{\sqrt{h}} \right) R_d \right] \quad (59)$$

$$b = \frac{1 - \left( 1 + \frac{1}{\sqrt{h}} \right) R_d}{2R_l - 1 + \left( 1 - \frac{1}{\sqrt{h}} \right) R_d} a \quad (60)$$

$$c = \frac{1 - \left( 1 - \frac{1}{\sqrt{h}} \right) R_d}{2R_l - 1 + \left( 1 - \frac{1}{\sqrt{h}} \right) R_d} a \quad (61)$$

$$d = \frac{2R_l - 1 + \left( 1 + \frac{1}{\sqrt{h}} \right) R_d}{2R_l - 1 + \left( 1 - \frac{1}{\sqrt{h}} \right) R_d} a \quad (62)$$

$$e = \frac{1 - R_d}{2R_l - 1 + \left( 1 - \frac{1}{\sqrt{h}} \right) R_d} a \quad (63)$$

$$f = \frac{2R_l - 1 + R_d}{2R_l - 1 + \left( 1 - \frac{1}{\sqrt{h}} \right) R_d} a \quad (64)$$

It is clear that for a given damage, i.e., fixed values of  $R_l$ ,  $R_d$  and  $h$ , Eq. (58) is a transcendental equation with only one unknown  $K_1 L$ . This equation can be easily solved by plotting the curve and locating the zero point.

After obtaining a solution of  $K_1 L$ , the natural frequency can be calculated according to Eq. (35):

$$f_d = \frac{(K_1 L)_n^2}{2\pi L^2} \sqrt{\frac{(EI)_1}{M_1}} = \frac{(K_1 L)_n^2}{2\pi 100^2} \sqrt{\frac{2.1 \times 10^{11}}{7000 \times 12}} = \frac{(K_1 L)_n^2}{2\pi \sqrt{40}} \text{ (HZ)}, \quad n = 1, 2, 3, \dots \quad (65)$$

The natural frequencies of the intact beam are (Humar 1990)

$$f = \frac{(n\pi)^2}{2\pi L^2} \sqrt{\frac{(EI)_1}{M_1}} = \frac{(n\pi)^2}{2\pi 100^2} \sqrt{\frac{2.1 \times 10^{11}}{7000 \times 12}} = \frac{(n\pi)^2}{2\pi \sqrt{40}} \text{ (HZ)}, \quad n = 1, 2, 3, \dots \quad (66)$$

To check the validity of the analytical solution, the results obtained from Eq. (65) will be compared with those from the ANSYS software. Letting  $R_l = 0.3$ ,  $R_d = 0.05$  and  $h = 0.5$  m, we use 200 two-node plane beam elements of length 0.05 m in the finite element model.

Table 1 shows the natural frequencies of the first ten modes. The analytical and FEM solutions agree well with each other. In addition, we observe that the natural frequencies do decrease due to damage. However, despite that the damage is large (for a real structure, the slot can be easily identified by naked eyes), the natural frequencies decrease by less than 3%. This minor difference can easily be masked by measurement errors in the modal test of practical structures, such as bridges or offshore platforms.

If we fix  $R_l = 0.3$  and change only  $R_d$  and  $h$ , we can calculate the  $K_1L$  value for the first mode as in Table 2. It is observed that: (1) with a fixed  $R_l$ , the value of  $K_1L$  decreases with  $h$ ; (2) for  $h$  greater than 0.5 m, the value of  $K_1L$  decreases with  $R_d$ ; and (3) for  $h$  less than 0.5 m, the value of  $K_1L$  first decreases upon the increase of  $R_d$ , and then increases when  $R_d$  is sufficiently large. This is due to the fact that the natural frequency depends on the structural stiffness and mass, and that the stiffness is proportional to  $h^3$ , while the mass is proportional to  $h$  and  $R_d$ . The implication from Table 2 is that noticeable changes in the natural frequency can be observed only if the damage is sufficiently large.

From the above discussion, it is clear that the natural frequencies do not change so much when a damage exists on the beam. If the damage changes the support condition, it can noticeably change the natural frequencies (Chondros and Dimarogonas 1980), but such a case is not covered by the present analytical solution. Moreover, the damage considered in this example is not an ideal crack but a notch, thereby excluding simulation of the singularity effect. However, this does not necessarily mean that small internal damages can substantially change the natural frequency, because even for ideal cracks, the change of natural frequency is regarded proportional to the square of the crack depth ratio, which is insignificant for most practical damage identification needs (Dimarogonas 1996).

### 3.2 Influence on mode shapes

After obtaining the value for  $K_1L$ , mode shapes can be calculated according to Eqs. (8) through

Table 1 Comparison of natural frequencies (in Hertz)

Mode		1	2	3	4	5
Intact		0.248	0.993	2.235	3.974	6.209
Damaged	FEM	0.243	0.967	2.229	3.928	6.036
	Theory	0.243	0.967	2.230	3.930	6.042
Mode		6	7	8	9	10
Intact		8.941	12.170	15.895	20.118	24.836
Damaged	FEM	8.860	12.103	15.477	19.786	24.731
	Theory	8.873	12.127	15.518	19.852	24.831

Table 2  $K_1L$  of the first mode for different damages ( $R_l = 0.3$ )

$R_d$	0.005	0.01	0.1	0.2	0.3	0.4	0.5	0.6	0.7
h									
0.05	1.139	0.962	0.558	0.495	0.483	0.496	0.522	0.543	0.547
0.1	1.865	1.594	0.933	0.824	0.797	0.806	0.838	0.862	0.867
0.2	2.697	2.449	1.543	1.355	1.295	1.289	1.309	1.328	1.332
0.3	2.980	2.849	2.029	1.789	1.697	1.669	1.674	1.684	1.686
0.4	3.073	3.009	2.401	2.146	2.034	1.987	1.978	1.981	1.982
0.5	3.109	3.078	2.672	2.440	2.319	2.261	2.240	2.236	2.236
0.6	3.125	3.110	2.857	2.671	2.559	2.496	2.469	2.463	2.462
0.7	3.133	3.125	2.980	2.848	2.756	2.700	2.672	2.663	2.661
0.8	3.138	3.133	3.060	2.979	2.917	2.873	2.850	2.842	2.841
0.9	3.140	3.138	3.110	3.074	3.044	3.019	3.007	3.001	2.999
1.0	$\pi$								

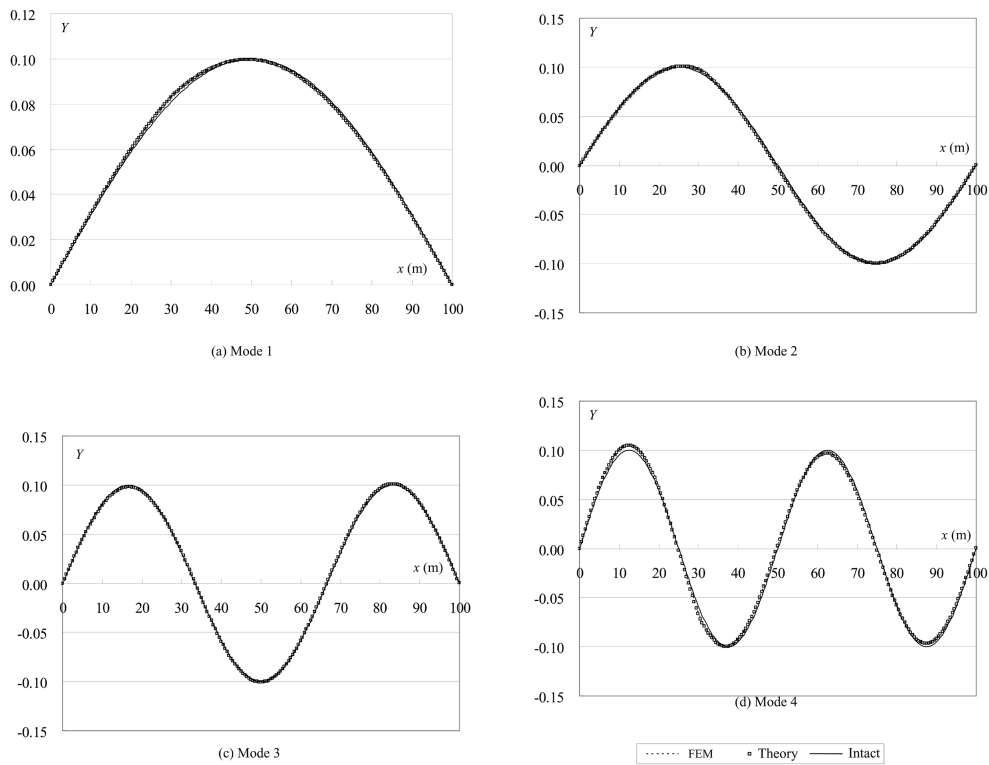


Fig. 3 Comparison of mode shapes

(10) and Eqs. (36) through (44). For the same simply-supported beam as in Section 3.1, with  $R_l = 0.3$ ,  $R_d = 0.05$  and  $h = 0.5$  m, we shall compare the analytical mode shapes obtained with the finite element results (with 200 two-node plane beam elements) and mode shapes of the intact beam

( $Y(x) = \sin\left(\frac{n\pi}{L}x\right)$ ,  $0 \leq x \leq L$ ,  $n = 1, 2, \dots$ , Humar 1990) in Fig. 3, in which all the mode shapes are

Table 3 Difference between damaged and intact mode shapes (%)

Mode	1	2	3	4	5	6	7	8	9	10
FEM	0.020	0.040	0.021	0.200	0.423	0.258	0.211	0.102	0.849	0.018
Theory	0.020	0.040	0.021	0.200	0.421	0.256	0.210	0.101	0.840	0.025

normalized to unity. As can be seen, the mode shapes from the analytical solution are almost the same as those from the finite element analysis, and that the mode shapes of the damaged beam differ slightly from the intact ones.

In modal testing, the measurement error  $\varepsilon_i$  of the  $i$ th mode shape is defined as

$$\varepsilon_i = \frac{\sum_{j=1}^N ({}^i Y_j^m - {}^i Y_j^*)^2}{\sum_{j=1}^N ({}^i Y_j^* {}^i Y_j^*)} = \sum_{j=1}^N ({}^i Y_j^m - {}^i Y_j^*)^2 \quad i = 1, 2, \dots, n \quad (67)$$

where  ${}^i Y_j^*$  and  ${}^i Y_j^m$  are the normalized true and measured values of the  $i$ th mode shape at point  $j$ , respectively, and  $N$  is the total number of measurement points. We can use Eq. (67) to indicate the difference between the damaged and intact mode shapes, as listed in Table 3 for the first ten modes. Because all the differences are less than 1%, it is generally difficult in practice to judge whether these are due to damage or measurement errors.

Another method for comparing two sets of mode shapes is the Modal Assurance Criterion (MAC) proposed by Allemang and Brown (1982). To compare the damaged and intact mode shapes, the MAC can be defined as

$$MAC_i = \frac{\left[ \sum_{j=1}^N ({}^i Y_j^{di} Y_j) \right]^2}{\sum_{j=1}^N ({}^i Y_j^{di} Y_j^d) \sum_{j=1}^N ({}^i Y_j^i Y_j)} = \left[ \sum_{j=1}^N ({}^i Y_j^{di} Y_j) \right]^2 \quad i = 1, 2, \dots, n \quad (68)$$

where  ${}^i Y_j^d$  and  ${}^i Y_j$  are the normalized values of the  $i$ th damaged and intact mode shape at point  $j$ , respectively. For  $R_l = 0.3$ ,  $R_d = 0.05$  and  $h = 0.5$  m, all the MAC values are greater than 0.98 (see Table 4). Therefore, it is not feasible to use the MAC values as a method for distinguishing between the damaged and intact mode shapes.

To locate the damage in a beam, Lieven and Ewins (1988) proposed the Coordinate Modal Assurance Criterion (COMAC), defined as

$$COMAC_j = \frac{\left( \sum_{i=1}^n |{}^i Y_j^{di} Y_j| \right)^2}{\sum_{i=1}^n ({}^i Y_j^{di} Y_j^d) \sum_{i=1}^n ({}^i Y_j^i Y_j)} \quad j = 1, 2, \dots, N \quad (69)$$

Table 4 MAC values: damaged and intact mode shapes ( $R_l = 0.3$ ,  $R_d = 0.05$ ,  $h = 0.5$  m)

Mode	1	2	3	4	5
FEM	0.999804	0.999601	0.999791	0.997997	0.995780
Theory	0.999804	0.999601	0.999792	0.998000	0.995790
Mode	6	7	8	9	10
FEM	0.997426	0.997891	0.989835	0.991532	0.999824
Theory	0.997438	0.997906	0.989907	0.991622	0.999748

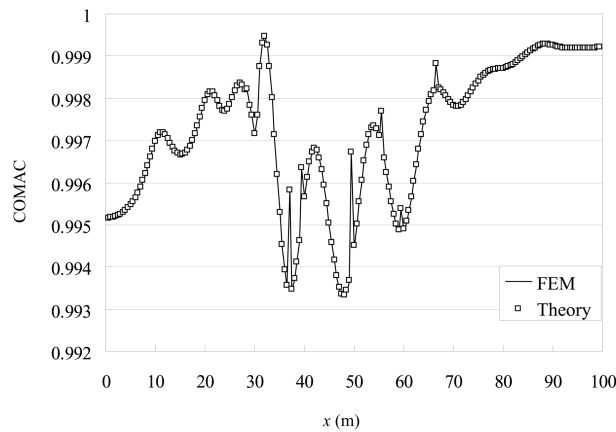


Fig. 4 COMAC values of damaged mode shapes

In Fig. 4, the COMAC values computed for the analytical and finite element mode shapes are plotted for  $R_l = 0.3$ ,  $R_d = 0.05$  and  $h = 0.5$  m. Clearly, this figure offers no new message for locating the damage.

From the above discussion, we can see that the mode shapes do not change so much when a damage exists on the beam. However, if the support condition was changed by a damage, a noticeable change in the mode shapes can be observed (Chondros and Dimarogonas 1980). Such a case was not covered by the present analytical solution.

### 3.3 Influence on the MRA

In Sections 3.1 and 3.2, we concluded that the natural frequencies and mode shapes are not very sensitive to damages not associated with the support conditions. Such an observation is consistent with the experiences of many researchers, who believe that a change of the local stiffness or mass due to damages do not have much effect on the global behaviors of the structure. Therefore, to find properties that are sensitive to damages, we should investigate some parameters that are representative of the local information.

One way to obtain local information is to take the derivative of the mode shapes over the spatial coordinate  $x$ . We realize that the first derivative of Eq. (8) through Eq. (10) explicitly contains damage information, because the parameters  $K_1$  and  $K_2$  will be extracted from the trigonometric functions by differentiation and the ratio of  $K_1$  over  $K_2$ , denoted as  $r$  (refer to Eq. (251)) relates directly to the severity of damage.

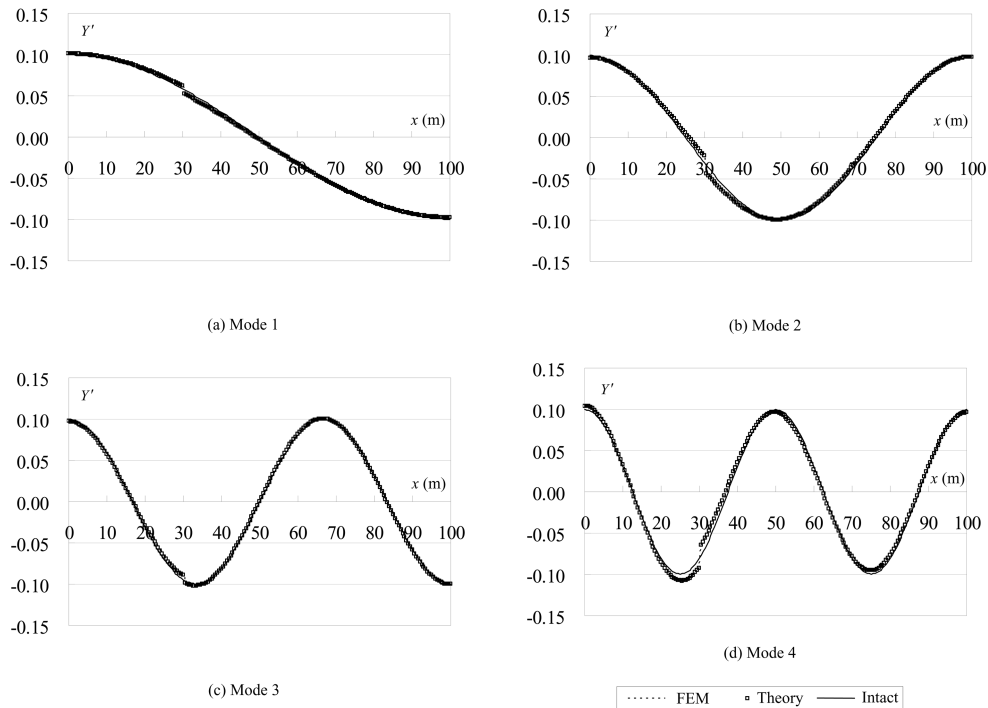


Fig. 5 Comparison of the MRA

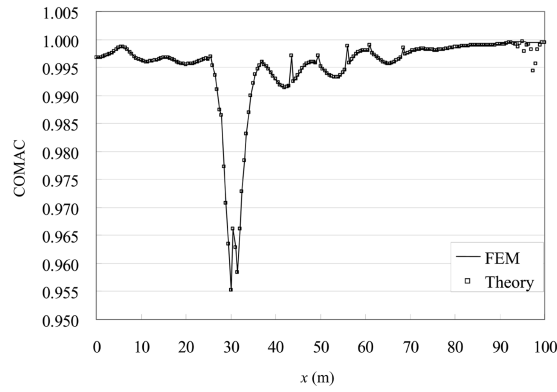
Table 5 MAC values: damaged and intact MRA ( $R_l = 0.3$ ,  $R_d = 0.05$ ,  $h = 0.5$  m)

Mode	1	2	3	4	5
FEM	0.998822	0.997688	0.999449	0.995425	0.990273
Theory	0.998822	0.997688	0.999449	0.995430	0.990287
Mode	6	7	8	9	10
FEM	0.995657	0.996530	0.981448	0.987683	0.999752
Theory	0.995671	0.996549	0.981544	0.987749	0.998484

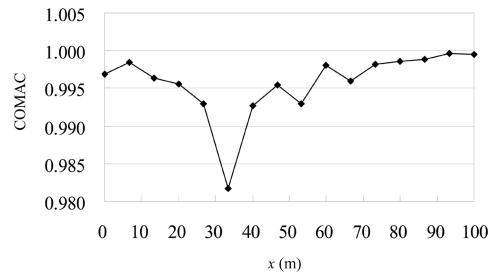
For the same simply-supported beam as in Section 3.1, we compare the normalized MRA of the damaged beam (with  $R_l = 0.3$ ,  $R_d = 0.05$  and  $h = 0.5$  m) and the intact beam. Both the analytical and finite element (200 two-node plane beam elements) results are plotted in Fig. 5, from which we can clearly observe the discontinuity on the curve of the damaged beam at the point of damage.

By replacing the mode shape with the MRA in Eq. (68), one can obtain the corresponding MAC values, as listed in Table 5 for the first ten modes. As can be seen, all the values are very high and not indicative of the existence of damage. Evidently, the MAC value is not a good index of damage because it is a global parameter.

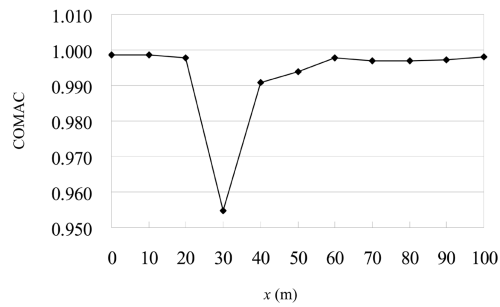
Fig. 6(a) depicts the normalized COMAC value of the MRA calculated at 201 points. The pulse of the curve clearly indicates the location of damage. In addition, to check the sensitivity of the MRA to damage, the normalized COMAC values with 16 and 11 points are plotted in Fig. 6(b) and 6(c), respectively. We observe that even with fewer points, it can still point out correctly the damage location. Of interest is that for the case of 16 points (see Fig. 6(b)), where no point is located at the



(a) 201 points



(b) 16 points



(c) 11 points

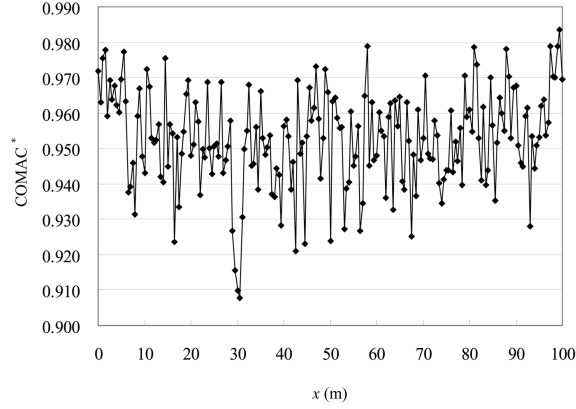
Fig. 6 COMAC values of damaged MRA free of noise ( $R_l = 0.3$ ,  $R_d = 0.05$ ,  $h = 0.5$  m)

damaged segment, the curve can still approximately show the existence of the damage location through its pulse.

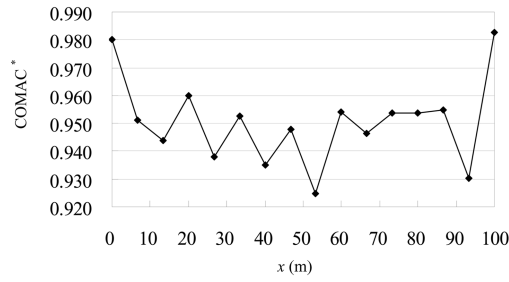
However, noise free measurements never exist in practical engineering. Using an equation similar to Eq. (67), the absolute measurement error at mode  $i$  can be estimated as

$${}^i\Delta = \sqrt{\frac{\varepsilon_i}{N}} \tag{70}$$

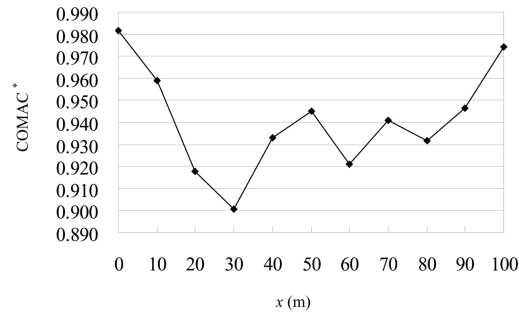
Thus the COMAC value of the polluted MRA can be expressed as:



(a) 201 points



(b) 16 points

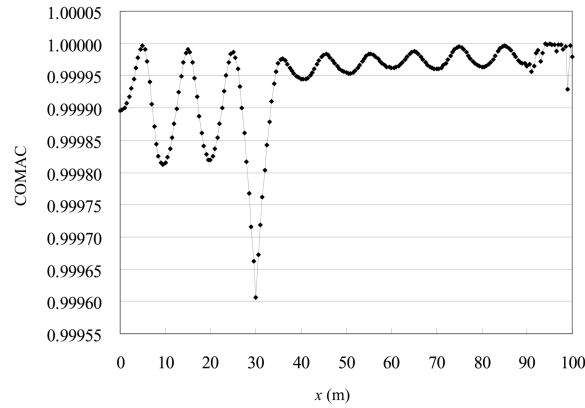


(c) 11 points

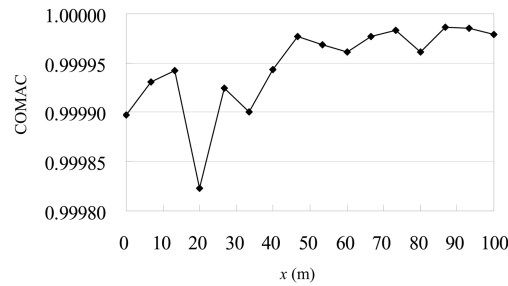
Fig. 7 COMAC values of polluted damaged MRA ( $R_l=0.3$ ,  $R_d=0.05$ ,  $h=0.5$  m)

$$COMAC_j^* = \left[ \sum_{i=1}^n |(iY_j^{d \pm i \Delta})^i Y_j^i| \right]^2 = \left[ \sum_{i=1}^n \left| \left( iY_j^{d \pm \sqrt{\frac{\mathcal{E}_i}{N}} \right)^i Y_j^i \right| \right]^2 \quad j = 1, 2, \dots, N \quad (71)$$

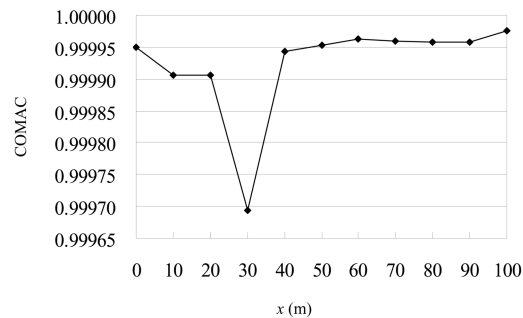
Supposing the measurement error is 5% for all modes, the corresponding COMAC values are depicted in Fig. 7. It is clear that the damage location can hardly be identified from these curves.



(a) 201 points



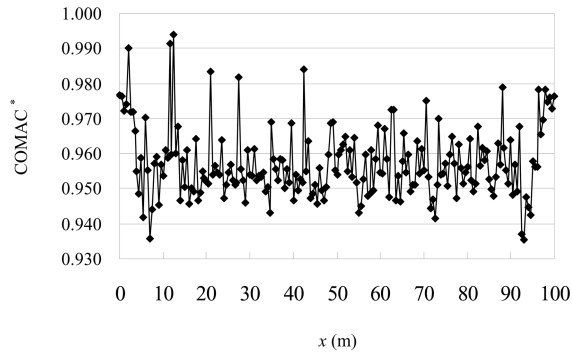
(b) 16 points



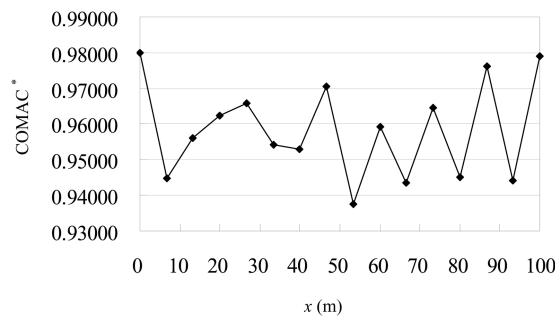
(c) 11 points

Fig. 8 COMAC values of damaged MRA free of noise ( $R_l = 0.3$ ,  $R_d = 0.05$ ,  $h = 0.9$  m)

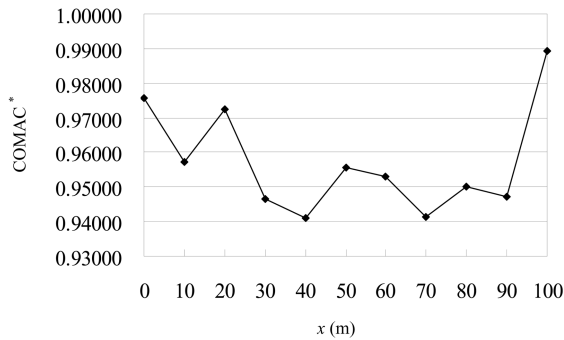
To further check the sensitivity of the MRA to damage, the analytical solution of a simply-supported beam with smaller damage ( $R_l = 0.3$ ,  $R_d = 0.05$  and  $h = 0.9$  m) is illustrated in the following. Fig. 8 shows the COMAC values free of measurement errors. We observe that although the COMAC value is very high, the damage location can be directly identified from the curve if some points are located in the damaged region. The curves in Fig. 9 are COMAC values plus a pollution of 5% measurement errors; it is clear that the damage information is masked by the noise.



(a) 201 points



(b) 16 points



(c) 11 points

Fig. 9 COMAC values of polluted damaged MRA ( $R_l = 0.3$ ,  $R_d = 0.05$ ,  $h = 0.9$  m)

### 3.4 Influence on curvature modes

Curvature modes are reported to be more sensitive to damages (Pandey *et al.* 1991). As a matter of fact, curvature modes are the second derivatives of the mode shapes. By taking the second derivatives to Eq. (8) through Eq. (10), the squares of  $K_1$  and  $K_2$  will be extracted from the

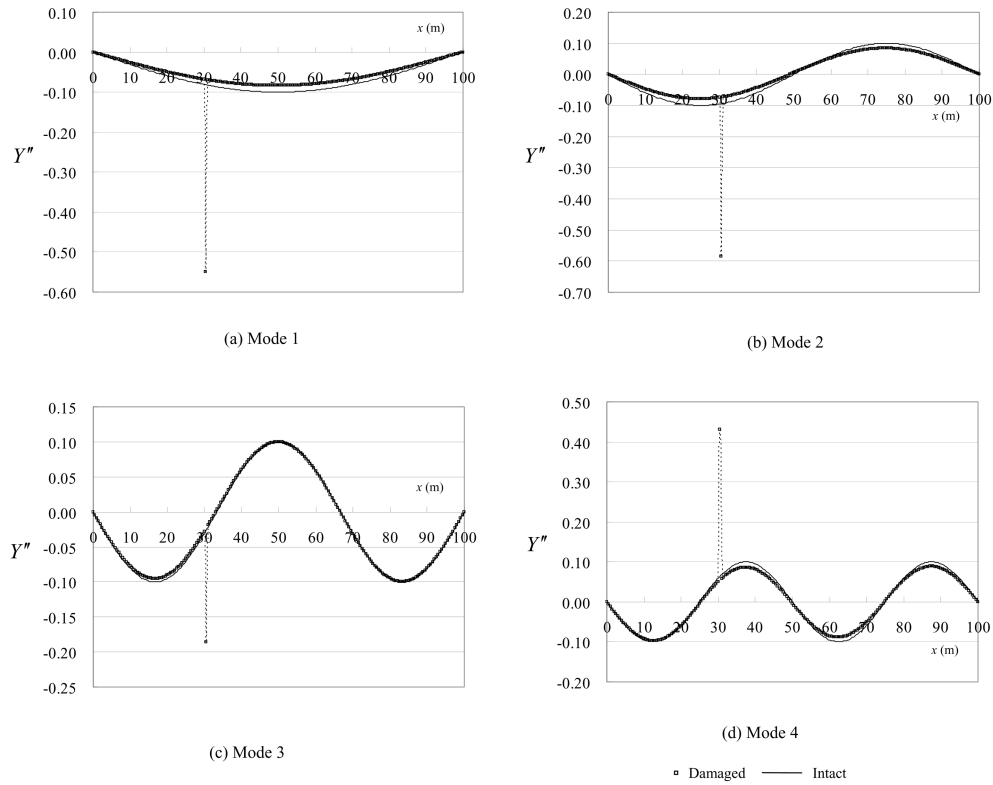


Fig. 10 Comparison of the curvature modes

trigonometric functions. The ratio of the square of  $K_1$  to that of  $K_2$  is  $r^2$ , which is more sensitive to damage than the parameter  $r$  itself. Therefore, curvature modes can be more sensitive to damages than the MRA. Such a conclusion is confirmed in the result of Fig. 10.

#### 4. Conclusions

This paper presents an analytical solution for the modal properties of simply-supported plane Euler-Bernoulli beams with a single damage. Based on this solution, we discuss extensively the sensitivities of the natural frequencies, mode shapes, MRA and curvature modes to damage. We observe that the natural frequencies and mode shapes are not very sensitive to internal damages while the MRA and especially the curvature modes are more sensitive to damages. These observations are consistent with the experiences of many researchers. The merit of this paper is to provide an analytical proof for all these observations. Based on this work, it is concluded that successful damage detection methods should be based on damage-sensitive dynamic properties which can properly reveal some local information.

Because curvature modes involve the second derivative of mode shapes, they serve as a better choice for damage detection than the MRA. In practice, however, the MRA can be easily obtained by using high precision dynamic inclinometers, while the curvature modes are often calculated from

the mode shapes by central difference approximation, which usually requires the installation of more sensors on the structure. No matter which dynamic property is adopted, further work is still needed to filter out measurement errors so as to enhance the reliability of damage detection (Li *et al.* 2008).

## Acknowledgements

This work is supported by the National Science Foundation of China with grant number 10802040. Such a financial support is gratefully acknowledged.

## References

- Abdo, M. A. B. and Hori, M. (2002), "A numerical study of structural damage detection using changes in the rotation of mode shapes", *J. Sound Vibration* **251**, 227-239.
- Allemang, R. J. and Brown, D. L. (1982), "Correlation coefficient for modal vector analysis", *Proceedings of the 1<sup>st</sup> International Modal Analysis Conference*, Society for Experimental Mechanics, Orlando, 110-116.
- Carden, E. P. and Fanning, P. (2004), "Vibration based condition monitoring: a review", *Struct. Health Monitor.*, **3**, 355-377.
- Chondros, T. G. and Dimarogonas, A.D. (1980), "Identification of cracks in welded joints of complex structures", *J. Sound Vib.*, **69**, 531-538.
- Christides, S. and Barr, A. D. S. (1984), "One-dimensional theory of cracked Bernoulli-Euler beams", *Int. J. Mech. Sci.*, **26**, 639-648.
- Dimarogonas, A. D. and Paipetis, S. A. (1983), *Analytical methods in rotor dynamics*, Applied Science Publishers, London and New York.
- Dimarogonas, A. D. (1996), "Vibration of cracked structures: a state of the art review", *Eng. Fract. Mech.*, **55**, 831-857.
- Farrar, C. R. and Jauregui, D. A. (1998), "Comparative study of damage identification algorithms applied to a bridge: I. experiment", *Smart Mater. Struct.*, **7**, 704-719.
- Humar, J. L. (1990), *Dynamics of structures*, Prentice Hall, New Jersey.
- Li, Y. Q., Zhou, M. S., Xiang, Z. H. and Cen, Z. Z. (2008), "Multi-type sensor placement design for damage detection", *Interact. Multiscale Mech.*, **1**, 357-368.
- Lieven, N. A. J. and Ewins, D. J. (1988), "Spatial correlation of modespaces: the coordinate modal assurance criterion (COMAC)", *Proceedings of the 6<sup>th</sup> International Modal Analysis Conference*, Society for Experimental Mechanics, Kissimmee, 1063-1070.
- Mazanoglu, K., Yesilyurt, I. and Sabuncu, M. (2009), "Vibration analysis of multiple-cracked non-uniform beams", *J. Sound Vib.*, **320**, 977-989.
- Owolabi, G. M., Swamidias, A. S. J. and Seshadri, R. (2003), "Crack detection in beams using changes in frequencies and amplitudes of frequency response functions", *J. Sound Vib.*, **265**, 1-22.
- Patil, D. P. and Maiti, S. K. (2005), "Vibration analysis of multiple-cracked non-uniform beams", *J. Sound Vib.*, **281**, 439-451.
- Pandey, A. K., Biswas, M. and Samman, M. M. (1991), "Damage detection from changes in curvature mode shapes", *J. Sound Vib.*, **145**, 321-332.
- Rizos, P. F., Aspragathos, N. and Dimarogonas, A. D. (1990), "Identification of crack location and magnitude in a cantilever beam from the vibration modes", *J. Sound Vib.*, **138**, 381-388.
- Salawu, O. S. (1997), "Detection of structural damage through changes in frequency: a review", *Eng. Struct.*, **19**, 718-723.
- Sinha, J. K., Friswell, M. I. and Edwards, S. (2002), "Simplified models for the location of cracks in beam structures using measured vibration data", *J. Sound Vib.*, **251**, 13-38.
- Thomson, M. T. (1949), "Vibration of slender bars with discontinuities in stiffness", *J. Appl. Mech.*, **16**, 203-207.

- Wang, J. and Qiao, P. (2007), "Vibration of beams with arbitrary discontinuities and boundary conditions", *J. Sound Vib.*, **308**, 12-27.
- Yuen, M. M. F. (1985), "A numerical study of the eigenparameters of a damaged cantilever", *J. Sound Vib.*, **103**, 301-310.
- Zheng, D. Y. and Fan, S. C. (2001), "Natural frequencies of a non-uniform beam with multiple cracks via modified Fourier series", *J. Sound Vib.*, **242**, 701-717.
- Zou, Y., Tong, L. and Steven, G. P. (2000), "Vibration-based model-dependent damage (delamination) identification and health monitoring for composite structures - a review", *J. Sound Vib.*, **230**, 357-378.

## Appendix

When there is no damage ( $K_1 = K_2 = K$  and  $s = r = 1$ ) Eq. (34) becomes

$$\sin(KL)\sinh(KL) = 0 \quad (\text{A1})$$

Because  $\sinh(KL) \neq 0$ , it requires  $\sin(KL) = 0$ , this leads to the well-known solution for natural frequencies of simply-supported beams without damage (Humar 1990)

$$\omega_n = \frac{(n\pi)^2}{L^2} \sqrt{\frac{EI}{M}}, \quad n = 1, 2, 3, \dots \quad (\text{A2})$$

In this case, the mode shapes degenerate to those in the intact state. The proof follows Adding Eqs. (17) and (19) gives

$$(C_1 - C_2)\sinh Kl_1 - D_2 \cosh Kl_1 = 0 \quad (\text{A3})$$

Subtracting Eq. (19) from Eq. (17) gives

$$(A_1 - A_2)\sin Kl_1 - B_2 \cos Kl_1 = 0 \quad (\text{A4})$$

Adding Eqs. (18) and (20) gives

$$(C_1 - C_2)\cosh Kl_1 - D_2 \sinh Kl_1 = 0 \quad (\text{A5})$$

Subtracting Eq. (20) from Eq. (18) gives

$$(A_1 - A_2)\cos Kl_1 + B_2 \sin Kl_1 = 0 \quad (\text{A6})$$

Eq. (A3) through Eq. (A6) can be written in matrix form as

$$\begin{bmatrix} \sin Kl_1 & -\cos Kl_1 & 0 & 0 \\ \cos Kl_1 & \sin Kl_1 & 0 & 0 \\ 0 & 0 & \sinh Kl_1 & -\cosh Kl_1 \\ 0 & 0 & \cosh Kl_1 & -\sinh Kl_1 \end{bmatrix} \begin{Bmatrix} A_1 - A_2 \\ B_2 \\ C_1 - C_2 \\ D_2 \end{Bmatrix} = \mathbf{0} \quad (\text{A7})$$

Because the determinant of the coefficient matrix of Eq. (A7) equals one, it has only the zero solution, i.e.,  $A_1 = A_2$ ,  $C_1 = C_2$ ,  $B_2 = 0$  and  $D_2 = 0$ .

Similarly, subtracting Eq. (23) from Eq. (21) gives:

$$(C_2 - C_3)\sinh Kl_2 + (D_2 - D_3)\cosh Kl_2 = 0 \quad (\text{A8})$$

Adding Eqs. (21) and (23) gives

$$(A_2 - A_3)\sin Kl_2 + (B_2 - B_3)\cos Kl_2 = 0 \quad (\text{A9})$$

Adding Eqs. (22) and (24) gives

$$(C_2 - C_3)\cosh Kl_2 + (D_2 - D_3)\sinh Kl_2 = 0 \quad (\text{A10})$$

Subtracting Eq. (24) from Eq. (22) gives

$$(A_2 - A_3)\cos Kl_2 - (B_2 - B_3)\sin Kl_2 = 0 \quad (\text{A11})$$

Eq. (A8) through Eq. (A11) can be written in matrix form as

$$\begin{bmatrix} \sin Kl_2 & \cos Kl_2 & 0 & 0 \\ \cos Kl_2 & -\sin Kl_2 & 0 & 0 \\ 0 & 0 & \sinh Kl & \cosh Kl \\ 0 & 0 & \cosh Kl & \sinh Kl \end{bmatrix} \begin{Bmatrix} A_2 - A_3 \\ B_2 - B_3 \\ C_2 - C_3 \\ D_2 - D_3 \end{Bmatrix} = \mathbf{0} \quad (\text{A12})$$

Because the determinant of the coefficient matrix of Eq. (A12) equals one, it has only the zero solution, i.e.,  $A_2 = A_3$ ,  $B_2 = B_3$ ,  $C_2 = C_3$  and  $D_2 = D_3$ .